Article

Congestion Relief Services by Vehicle-to-Grid Enabled Electric Vehicles Considering Battery Degradation

Shashank Narayana Gowda [1,*] **, Hamidreza Nazaripouya** [2,3] **and Rajit Gadh** [1]

[1] Smart Grid Energy Research Center, University of California, Los Angeles, CA 90095, USA; gadh@ucla.edu

[2] Power Grid Modernization Lab, Oklahoma State University, Stillwater, OK 74075, USA; hanazar@okstate.edu

[3] Electrical and Computer Engineering Department, University of California, Riverside, CA 92521, USA

[*] Correspondence: shashank07@ucla.edu

Abstract: Battery electric vehicles (BEVs) offer substantial potential to enhance the electric grid through bi-directional charging technologies. In essence, BEVs, functioning as portable battery energy storage systems, play a pivotal role in enabling the seamless integration of renewable energy, grid optimization, and ancillary services. This article sets out to explore the value of BEVs equipped with Vehicle-to-Grid (V2G) for grid operators, particularly in the context of alleviating congestion. This valuable service, though not accompanied by direct monetary compensation for users, holds significant promise in minimizing congestion and renewable energy curtailment. This study utilizes the Day-Ahead Locational Marginal Price (LMP) data obtained from various locations within California Independent System Operator (CAISO) to ascertain the financial benefits to BEVs located on either side of congestion at different grid nodes, across various months. Similar analysis is performed on some of the largest solar energy plants in California. Mixed-integer linear programs are used to optimize the charging/discharging decisions for the BEV for maximizing revenue from LMP arbitrage and for minimizing the congestion component of LMP. Additionally, we take into account the impact of battery degradation, quantified as a cost per kilowatt-hour ($/kWh), and integrate this factor into our assessment to understand the evolving discharging behavior of BEVs. The article compares the benefits from the BEVs towards congestion minimization for the two different optimization scenarios, discusses seasonality, and addresses the importance of adequately compensating BEV users and incentivizing them to prioritize congestion relief during specific time intervals.

Keywords: electric vehicles; V2G; congestion relief; battery degradation; LMP

1. Introduction

The growing integration of intermittent renewable energy sources (RES), such as solar and wind, alongside the increasing adoption of battery electric vehicles (BEVs) as part of the global effort to combat climate change and reduce air pollution has presented notable challenges in the effective management and stability of our energy grid [1]. Shifting our electric grid towards a greater reliance on RES and electrifying our transportation to meet sustainability goals demands effective instruments and markets to maintain grid equilibrium across all timeframes. Among the promising solutions supporting this transition are battery energy storage systems (BESS), thanks to declining costs and extended battery lifespans [2].

Grid-scale BESS stands out as a versatile option, capable of swiftly and economically storing and supplying substantial energy quantities, often in the range of megawatt-hours (MWh), all while maintaining high efficiency, reliability, and safety standards [3]. The potential of BESS is multifaceted, offering benefits to Independent System Operators (ISOs), Regional Transmission Organizations (RTOs), utilities, and end-users alike [4]. For instance, behind-the-meter (BTM) energy storage can ensure backup power, optimize the utilization of solar photovoltaics (PV), reduce electricity expenses through time-of-use (TOU) pricing

schemes, and engage in peak shaving for both residential and commercial consumers [5]. Moreover, BESS has the capacity to minimize load variance [6], lower electricity costs by mitigating RES curtailment [7], and facilitate electric bus charging, ultimately reducing demand charges [8].

BESS can also harness fluctuating electricity prices in Day-Ahead Markets (DAM) and Real-Time Markets (RTM) to generate revenue through arbitrage, a strategy that involves charging batteries at low prices and discharging at high prices [9]. Additionally, BESS can participate in ancillary services, such as voltage support, reserves [4], frequency regulation [9], and reactive power compensation [10], across different jurisdictions, depending on local regulations and market dynamics. Furthermore, BESS can yield savings through deferring costly transmission grid upgrades, distribution grid enhancements, and by providing congestion relief [4].

BEVs present another dimension in this evolving landscape. BEVs rely exclusively on the energy stored in their batteries for transportation and have the advantage of emitting fewer greenhouse gases (GHGs) when charged with RES compared to internal combustion engine vehicles [11]. Coordinated smart charging of BEVs further reduces the cost per mile driven [12]. Data from the US Department of Transportation's National Household Travel Survey (NHTA) suggests that, on average, private vehicles spend a mere 4% of their day in active use [13]. This leaves substantial room for BEVs to provide grid services when plugged in, especially considering their compatibility with the innovative concept of Vehicle-to-Grid (V2G) technology [14].

With V2G capabilities, BEVs can facilitate two-way communication and power flow with the grid, effectively enabling them to function as backup power sources [15]. Coordinated energy management of BEVs enhances grid efficiency, performance, and power quality [16] while minimizing charging costs. Parked and plugged-in BEVs have the potential to generate revenue by offering grid services like frequency regulation [17] and voltage regulation or by participating in energy arbitrage with TOU pricing [18]. Furthermore, BEVs can charge with excess renewable energy and supply that energy back to the grid during periods of need, thus reducing curtailment and alleviating peak load, particularly in regions with distinctive load profiles, such as California's notorious "duck curve" [19]. BEVs contribute not only to lower emissions from vehicles but also to reduced emissions from peaking power plants through their V2G capabilities [20]. The practical connection between the BEV and the electric grid for V2G has not been discussed in this work. More details on EV-grid integration, grid-connection standards, bidirectional/unidirectional charger topologies, and V2G operation are explored in review articles [21,22].

As of 2021, numerous BEV models boast impressive battery energy capacities exceeding 90 kWh and power transfer capabilities exceeding 250 kW [23]. However, the rate of power transfer remains constrained by the internal power circuitry of the BEV and manufacturer-imposed limitations. The increasing popularity of BEVs and the potential financial incentives stemming from V2G technology are poised to motivate more BEV manufacturers to embrace bidirectional power flow, driven both by economic and environmental considerations. Despite the extensive exploration of BESS and BEVs with V2G in numerous electric grid applications, one aspect that remains relatively uncharted is the potential of BEVs with V2G to alleviate congestion. The prospects here are significant, with the potential to realize substantial monetary savings, such as the case in CAISO, where BEVs assisting in transmission congestion relief could result in monthly savings of up to $280.47 [24]. However, it is essential to recognize that this work assumed constant BEV availability for grid support, treated BEVs as small batteries, and did not account for the effects of battery degradation.

This article aims at projecting the benefits of BEVs providing congestion-related cost minimization in the current aging electric grid infrastructure. The charging/discharging strategies used by BEVs for congestion relief and arbitrage are explored at different locations in the California Independent System Operator (CAISO) jurisdiction. The battery degradation experienced by the BEVs is modeled as a constant degradation cost factor.

This study focuses on the nodes at the ends of some of the most congested lines as well as some of the largest solar generation plants in California to explore the value of BEVs supporting congestion relief for a multi-year time frame. We explore the temporal benefits on a monthly basis at these key points by using locational marginal pricing (LMP) data and study the trade-off between minimizing congestion and maximizing arbitrage revenue. To the best of our knowledge, we are the first to explore the value of BEVs on congestion relief in this manner by identifying existing congested transmission lines and large solar plants and utilizing real pricing data. By participating in this form of congestion minimization, BEVs can charge to potentially minimize the curtailment of cheaper sources of sustainable energy like solar and discharge energy locally to offset the use of more expensive polluting peaker plants, thereby minimizing pollution.

The subsequent sections of this paper are structured as follows: Section 2 provides a comprehensive overview of congestion relief, financial transmission rights, and locational marginal prices. Following this, we discuss the node selection process, battery degradation models, and the optimization programs for minimizing total cost and congestion-related costs. In Section 3, we present the results of the optimization programs at each node as a total value of each BEV for congestion minimization and break it down on a monthly basis as well. We also look at battery degradation in terms of capacity loss and the value per unit of V2G. In the final Section 4, we discuss our findings and outline prospective directions for future research.

2. Materials and Methods

2.1. Congestion Relief and Financial Transmission Rights

Line congestion arises when the existing transmission lines face limitations due to thermal, voltage, or stability constraints. These constraints result in congestion pricing in various electricity markets in some countries, incurring costs for operating transmission lines near their capacity [25]. Such congestion can hinder the efficient flow of electricity from low-cost sustainable RES to end-users. Consequently, more expensive generation sources are turned on to send the required energy across non-congested lines, driving up electricity prices in the affected areas. This phenomenon triggers alterations in LMPs at specific nodes within the electric grid network [26].

To mitigate the uncertainty and variability of transmission prices stemming from congestion, electricity markets establish agreements between system operators and market participants known as Financial Transmission Rights (FTR) [27]. FTRs are typically issued through auctions and allocations in the financial transmission market, with allocation determined by the simultaneous feasibility within the market's security-constrained optimal power flow problem [28]. FTRs grant holders the entitlement to payments equal to the energy price differential between the source and sink nodes for each transported megawatt-hour (MWh) of energy for a given transmission line. When lines become congested, congestion rents are collected by the ISOs and distributed among FTR holders [27].

However, challenges persist within the FTR market. Notably, FTRs do not resolve physical congestion; they remain a financial instrument. Furthermore, each regional ISO operates with its distinct rules and regulations for potential FTR market participation, potentially excluding entities that require protection against congestion costs. Even approved participants may face difficulties in auctions. In ideal conditions, if transmission constraints are unviolated, FTR allocation should mirror electricity flow in the Day-Ahead Market, guaranteeing that FTR payouts equal auction revenue [29]. Nevertheless, real-world scenarios often deviate from this ideal, leading to underfunding. FTR underfunding reflects a revenue shortfall when collected LMP congestion costs fall short of the credits distributed to FTR holders [30]. This problem has persisted across various ISOs for years, with instances like PJM (Pennsylvania Jersey Maryland RTO) experiencing FTR underfunding as high as 31% in 2012–2013 and 28% in 2013–2014, while the SPP (Southwest Power Pool) ISO reported 20% underfunding in 2014–2015 with monetary values in the range of tens of millions of dollars.

The design of FTRs involves bilateral contracts with transmission charges associated with each transaction between injection and withdrawal points, based on the price disparity between these nodes [31]. Typically, loads pay the LMP at the point of withdrawal, while generators receive the LMP at the point of injection for each additional MWh. Both nodes incur congestion fees when the LMPs at these points differ. The ISO, which collects congestion rents, reimburses the FTR holders accordingly. FTRs go by different names in various regions, such as Congestion Revenue Rights (CRR) in California and Transmission Congestion Contracts (TCC) in New York, with variations mainly arising in contract design, duration, acquisition methods, trading, auction mechanisms, allocation criteria, and revenue distribution [31].

Regulation plays a vital role in the FTR market, as unchecked dominance within it can incentivize generation curtailment and inflate FTR values [32]. Minimizing congestion rent is a potential solution to address the inefficiencies of the FTR market. Achieving this goal could involve leveraging energy storage or V2G to alleviate transmission congestion, ultimately enhancing the utilization of existing grid assets.

2.2. Utility Scale Energy Storage Projects for Congestion Relief

There have been attempts to study the use of energy storage to minimize transmission grid congestion without looking into FTRs. Del et al. used battery energy storage to relieve thermal constraints and hence provide congestion relief [33]. Khani et al. developed a Real Time Optimal Dispatch (RTOD) algorithm for privately owned large scale BESS. This allowed BESS to generate revenue primarily by arbitrage in the Day-Ahead Market and also prepared the BESS to maximize contribution to congestion relief as an ancillary service [34]. Arteaga et al. researched the potential for BESS to compete in an electricity market to trade energy and provide ancillary services. The BESS also has an opportunity to provide transmission congestion relief (TCR) under a long-term contract with a regional network operator [35]. They modelled the opportunity costs (difference between maximum profit with and without TCR) for TCR with the limitations imposed on participating in the electricity markets while providing TCR. The DOE (Department of Energy) Global Energy Storage Database also contains information on grid-connected energy storage projects used for transmission congestion relief [36]. Globally, there are 26 operational battery storage projects that are used for transmission congestion relief, with 9 of them in the USA. Table 1 provides key information on the energy storage projects used for transmission congestion relief in the USA.

Table 1. Grid-scale battery projects in the USA resulting in transmission congestion relief.

Project Name	Rated Power (kW)	Storage Capacity (kWh)	State	City
Long Island Bus BESS—New York Power Authority	1000	6500	New York	Garden City
Redding Electric Utilities (Phase 1)—Ice Energy	1000	6000	California	Redding
SustainX Inc Isothermal Compressed Air Energy Storage	1500	1500	New Hampshire	Seabrook
Tehachapi Wind Energy Storage Project	8000	32,000	California	Tehachapi
Glendale Water and Power/Skylar Energy BESS Pilot	2000	960	California	Glendale
University of Hawaii Smart Grid Regional and Energy Storage Demonstration Project (Maui Smart Grid)	1000	1000	Hawaii	Wailea
PDE Smart Microgrid System	90	29.7	California	Commerce
Borrego Springs Microgrid—SDG&E	500	1500	California	Borrego Springs
Redding Electric Utilities (Phase 2)—Ice Energy	6000	12,000	California	Redding

With respect to BEVs, Staudt et al., evaluated the effect of uncontrolled BEV charging on the expansion of the German transmission grid and proposed a coordinated charging approach to relieve the transmission grid of congestion [37]. In order to calculate possible compensation for participants, they reduced their model to one node per state. Refer-

ence [38] developed a Day-Ahead Market framework for congestion management by using a decentralized mechanism for the collaboration of BEV aggregators that utilized BEVS as distributed storage. Their work focused on day-ahead congestion and ran their simulations for only 24 h time periods in an unbalanced 136 bus system. Gowda et al. claimed that BEVs supporting transmission congestion relief can lead to monetary savings as high as $280.47 in one month in CAISO [24]. This work was based on the assumption that each BEV was always available to support the grid and treated the BEV as a small battery and ignored the effects of battery degradation.

2.3. Locational Marginal Price

The LMP represents the price of electricity at a specific location on the electric grid at any point in time. The total LMP_T can be broken down into 3 components—energy, congestion, and loss, as shown in Equation (1). Here, LMP_E, LMP_C, and LMP_L represent the energy component, congestion component, and the loss component.

$$LMP_T = LMP_E + LMP_C + LMP_L \tag{1}$$

LMP_C is positive when congested transmission lines do not allow electricity from cheaper sustainable sources of energy (like renewables) to reach a node, resulting in the usage of nearby or local higher-cost non-renewable sources to meet the demand, resulting in increased energy prices and pollution. LMP_C is negative when there is excess transmission capacity at a location but little demand for electricity, leading to the under utilization of sustainable sources of energy like RES. The difference between the congestion components of the LMPs of two nodes is the congestion charge in moving energy between them [26]. The price of moving E MWh of energy between the source and sink node is given by Equation (2).

$$C_{FTR} = E(LMP_{C,\text{sink}} - LMP_{C,\text{source}}) \tag{2}$$

FTRs allow settlements based on the difference between source and sink congestion prices when the transmission line between them is congested in the Day-Ahead Market. In CAISO, FTRs are called CRRs. Load Serving Entities (LSE) can become CRR holders if they meet any of three minimum conditions—(1) $1 million tangible net worth, (2) $10 million total assets, or (3) post financial $500,000 cash or letter of credit. Completing the required applications is followed by registration, agreement policies, and training to obtain CRR. Each ISO have their own criteria to become FTR holders. As mentioned previously, FTRs protect a limited number of entities against price stochasticity, and the physical lines connecting nodes are still congested.

In the following section, the maximum monetary benefits that could be obtained by a single BEV at various nodes at the ends of congested lines and at large solar generation plants in CAISO from March 2021 to September 2023 is presented. The required LMP data to plug in the mathematical models are obtained from CAISO using the gridstatus module in Python. With a larger range of time data, we can study the effect of seasonality as well as the effect of the increase in renewable energy installed in the grid. The node selection process is discussed next.

2.4. Node Selection Process

CAISO releases a market performance report for each month, and the reports from 2021 onwards are available on their website [39]. The market performance report discusses trends in system peak load, resource adequacy, day-ahead and real-time prices, congestion, CRRs, and ancillary services. These reports discuss congestion rents on interties, transmission lines, transformers, nomograms, and nodal group constraints. The following three transmission lines show up often in the reports from March 2021 to September 2023, (1) 230 kV line between Panoche and Gates, (2) 500 kV line between Los Banos and Gates, and (3) 230 kV line between Gates and Midway. The locations of these transmission lines were identified from the California Electric Transmission Lines dataset hosted on the Cali-

fornia State Geoportal [40]. The ends of the transmission lines were identified and mapped with the nodes on the price map provided by CAISO [41]. The nodes at the two ends of the transmission lines are shown in Table 2.

Table 2. Congested transmission lines and nodes at the ends of the transmission lines.

Transmission Line	Nodes
230 kV Panoche–Gates	DGPAN1_7_B1, HURON_6_N001
500 kV Los Banos–Gates	SNTANLA_6_N001, HURON_6_N001
230 kV Gates–Midway	HURON_6_N001, MIDWAY_1_N047

Additionally, nodes representing 5 of the largest solar PV plants in California are chosen to study the potential for V2G to minimize congestion losses and potentially mitigate sustainable energy curtailment. The locations of these power plants were identified from the California Power Plants dataset hosted on the California State Geoportal [42]. The solar power plants were filtered based on capacity (250 MW or greater), status (not retired), and location (power plants near borders were excluded). The locations of these solar power plants were identified and mapped with the nodes on the price map provided by CAISO [41]. The names, capacity, and nodes of these solar power plants are shown in Table 3.

Table 3. Chosen solar power plants from California for analysis.

Name	Capacity (MW)	Node
Topaz Solar Farm	550	TOPAZC1_7_N021
Antelope Valley Solar	250	AVSOLAR_7_N008
Desert Stateline Solar Facility	300	DSRTHV3_7_N003
California Valley Solar Ranch	250	CAVLSRGN_7_B1
Genesis Solar Energy Project	250	TOT223L2_7_N001

2.5. LMP Visualization

In this section, we will observe some of the characteristics of the LMPs at the chosen nodes. We focus on one transmission line and the nodes at the ends of it, as well as one node from the solar power plants for brevity. Typically, the units of LMP are $/MWh, but we plot them as $/kWh since the charging/discharging rate from the BEV are in the order of kW.

In Figure 1, we can observe the energy component of LMP and the congestion component of LMP plotted across the given time frame (March 2021 to September 2023) for the node DGPAN1_7_B1. LMP_E is the average LMP for the entire grid and reflects, on average, the cost to add the next unit (MWh) of energy into the grid. We observe that LMP_E is mostly positive and generally higher in the summer months each year. Figure 1 also shows that there was a higher LMP_E in the winter months of December 2022 until March 2023. Meanwhile, at this particular node, LMP_C is negative most of the time and is mostly positive in the months of December 2022 until March 2023. We can observe that there are instances where it makes sense to charge the BEV during time intervals with high LMP_E when the LMP_C is low to minimize congestion or renewable energy curtailment. We will delve into details in future sections.

Figure 2 shows the congestion components of LMPs at the two nodes at the ends of the transmission line 230 kV Panoche–Gates. It can be seen on multiple points in the chosen time frame that BEVs at the nodes need to perform the opposite task if the goal is to minimize congestion. During the month of December 2022, we would expect the BEVs at node HURON_6_N001 to charge at certain hours, while the BEVs at node DGPAN1_7_B1 would discharge at the same hours. The optimized actions of BEVs will be discussed in future sections.
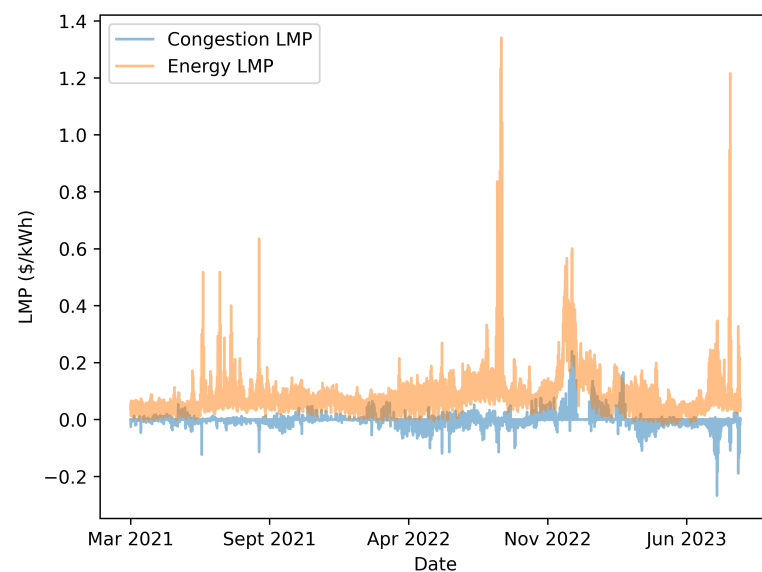
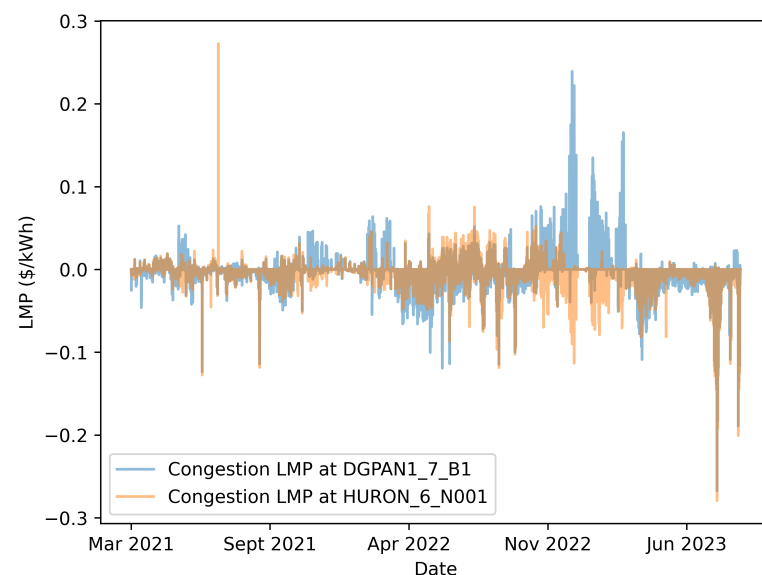**Figure 1.** Congestion and energy components of LMP visualized for DGPAN1_7_B1.

Figure 2. Congestion components of LMP visualized for the ends of the 230 kV Panoche–Gates transmission lines at nodes DGPAN1_7_B1 and HURON_6_N001.

Finally, we look at Figure 3 to observe LMP_C at large solar power plants. We can see that LMP_C is predominantly negative. We see that there is a seasonal component to it. LMP_C is largely negative during the spring months of the year, and some positive spikes in LMP_C can be observed during summer. This indicates seasonal curtailment in renewable energy in the nodes near the solar power plants due to lack of demand. However, existing transmission capacity does not allow for this energy to be transported to other nodes, perhaps due to a lack of demand.

CAISO provides data on renewable energy curtailment each year [43]. With increasing penetration of renewable energy in the grid, the curtailment in the months of February to June for both 2022 and 2023 have been over 200,000 MWh. In 2021, the maximum amount of curtailment occurred in the month of March, about 240,000 MWh. In 2023, the curtailed energy in the month of March almost tripled to 700,000 Mwh. By potentially creating markets that incentivize electricity consumption at local nodes based on congestion pricing,

sustainable energy curtailment and reliance on expensive polluting power plants could be minimized.
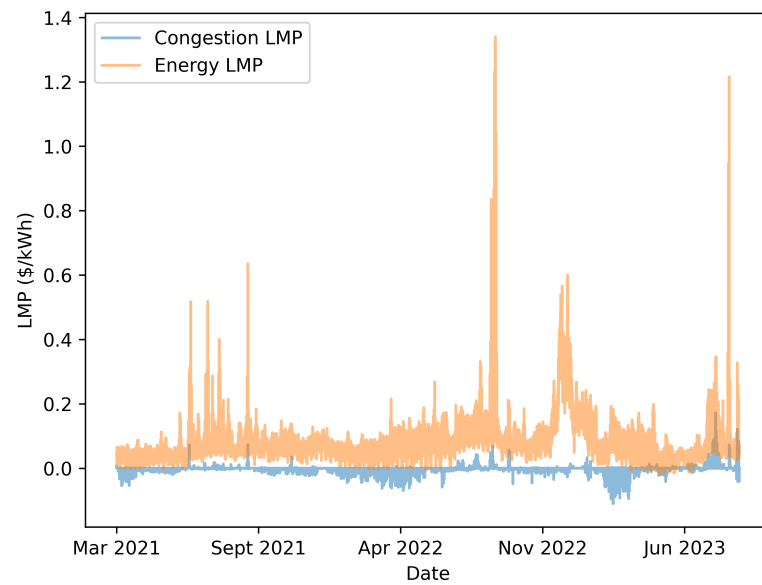

Figure 3. Congestion and energy components of LMP visualized for DSRTHV3_7_N003.

2.6. Battery Degradation

Participation in V2G applications reduces the service life of the batteries housed by BEVs due to the increased number of charging cycles. There are multiple approaches that have been used to account for battery degradation in V2G, like equivalent circuit models, electrochemical models, performance based models, neural networks, and so on [44]. In our case, we choose to use a degradation model represented as a constant degradation cost factor that can be directly utilized in the objective function of the optimization model [45]. While battery degradation consists of both calendar and cyclic aging, we focus on the capacity loss purely due to the increased cycles and ignore the degradation that occurs from calendar aging. This enables the use of a constant degradation parameter in the optimization objective instead of a variable degradation parameter that depends on the current state of health of the battery [18]. Our battery degradation model is based on recent work in [44] that describes a weighted Ah-throughput model (wAh model) using a constant degradation cost factor.

The wAh model used here is based on curve fitting performed on measured experimental data in [46]. The fitting function describing capacity loss C_{loss} is shown in Equation (3).

$$C_{loss} = k_C k_D f^{1/2} \tag{3}$$

In Equation (3), k_C describes the influence of C-rate and k_D describes the influence of depth of cycle (DoC). f represents the number of full equivalent cycles. The fitting functions of k_C and k_D are described in Equations (4) and (5), respectively.

$$k_C = 0.063 C_{rate} + 0.0971 \tag{4}$$

$$k_D = 4.0253(DoC - 0.5)^3 + 1.0923 \tag{5}$$

k_C is a linear function of the C-rate of the battery, and k_D depends non-linearly on the depth of cycle. f is a function of cell capacity C_{cell} and charge quantity throughput Q, as shown in Equation (6).

$$f = \frac{Q}{2C_{cell}} \tag{6}$$

The battery cell under consideration has a nominal capacity (C_{cell}) of 2.85Ah. The effect of temperature on degradation is ignored since BEVs are equipped with a Battery Thermal Management Systems (BTMS) that ensure that the battery pack operates at an optimal range [46]. Ref. [47] reviews the latest advancements in BTMS for BEVs and discusses in detail how combinations of passive and active cooling/heating methods are used by BTMS to meet the stringent thermal requirements.

The opportunity cost from battery aging is determined using the initial cost of the battery, assuming that the battery is valued at 0\$ when it reaches the end of its life at 20% capacity loss (or 80% of its initial capacity). The specific price of the battery pack C^{inv} is set at \$118/kWh based on [44]. With this information, we can obtain a constant degradation cost factor CF_{deg} in \$/kWh using Equation (7).

$$CF_{deg} = \frac{C^{inv} E^{rat}}{E^{life}} \tag{7}$$

E^{rat} is the rated capacity of the battery, and E^{life} is the maximum possible lifetime energy throughput until the battery reaches the end of its life. E^{life} can be computed using Equation (8) by utilizing Equation (3) and the fact that the battery is valued at 0\$ at 20% capacity loss.

$$E^{life} = 2E^{rat}(\frac{20\%}{k_C k_D})^2 \tag{8}$$

The constant degradation cost factor CF_{deg} will be directly utilized in the objective of the optimization problem. We estimate the CF_{deg} for a Nissan Leaf BEV with a battery capacity 40 kWh that can be charged/discharged at 6.6 kW using the described methodology as 0.18 cents/kWh.

2.7. Optimization

At each node under consideration, we optimize for two outcomes. Firstly, we use a Nissan Leaf BEV for the minimization of the congestion component of the LMP at the node and then for the minimization of the total LMP at the node by means of charging and V2G. Minimization of the congestion component results in greater utilization of local cheaper sustainable energy, and potential reduction in sustainable energy curtailment and stress on transmission lines. The minimization of total LMP results in maximum revenue or minimum charging cost to the BEV by trading energy at the appropriate times. Here, we only look at the benefits to a single BEV and the tradeoff between the outcomes with these two methods. The usage of a large number of BEVs for V2G (hundreds of kW or MW) can potentially update the LMPs significantly and drastically affect the power flow in the entire grid. Hence, we pick a single BEV for our analysis to identify the value that it brings to congestion relief.

For our study, we consider a Nissan Leaf with a battery capacity of 40 kWh that can be charged/discharged at at a maximum rate of 6.6 kWh with 90% efficiency. We assume that the minimum possible state of charge of the BEV is 10% and a maximum possible state of charge is 90%. Within these constraints, the charging or discharging profile is assumed to be linear. Time is discretized into hourly intervals, and we work with a simple uncertainty that the BEV is not available for charging or V2G for a one hour interval interval between 8–10 AM, as well as another hour between 4–6 PM to be used for transportation, creating 4 scenarios typical for an average workday. The minimized congestion-related costs or charging costs, the total energy discharged by the BEVs, the battery degradation, and the \$ value per kWh of discharge is calculated at each of the nodes for all the months between March 2021 to September 2023 and reported as an average value from all scenarios. We

also assume that the BEVs do not travel far enough to another node's service area. The optimization problem is described below.

$$\text{Minimize} \quad \sum_{k=1}^{T}(LMP_{i,k}(P_{ch,k} - P_{dch,k}) - CF_{deg}(P_{ch,k} + P_{dch,k}))\Delta_T \tag{9}$$

subject to

$$E_k = E_{k-1} + (P_{ch,k}\eta_{ch} - P_{dch,k}/\eta_{dch} - P_{driv,k})\Delta_T \quad \forall k \in \{T\} \tag{10}$$

$$E_{min} \le E_k \le E_{max} \quad \forall k \in \{T\} \tag{11}$$

$$0 \le P_{ch,k} \le \delta_{ch,k}P_{ch,max} \quad \forall k \in \{T\} \tag{12}$$

$$0 \le P_{dch,k} \le \delta_{dch,k}P_{dch,max} \quad \forall k \in \{T\} \tag{13}$$

$$\delta_{ch,k} \in \{0,1\} \quad \forall k \in \{T\} \tag{14}$$

$$\delta_{dch,k} \in \{0,1\} \quad \forall k \in \{T\} \tag{15}$$

$$\delta_{ch,k} + \delta_{dch,k} \le 1 \quad \forall k \in \{T\} \tag{16}$$

$$\delta_{ch,k} = 0 \quad \forall k \in \{T_{driv}\} \tag{17}$$

$$\delta_{dch,k} = 0 \quad \forall k \in \{T_{driv}\} \tag{18}$$

$$E_k \ge E_{dep,k} \quad \forall k \in \{T_{dep}\} \tag{19}$$

The optimization problem is formulated as a mixed integer linear program (MILP) that is run multiple times for each node for all the months chosen (with no change in timings of EV departure, arrival, and energy consumed driving). The day-ahead LMP data including the 3 components—energy, congestion, and loss for every time interval at each node—is obtained using the gridstatus module in Python. Equation (9) states that the objective function minimizes the charging cost with $LMP_{i,k}$ using the BEV with V2G. The i in $LMP_{i,k}$ can be T, with $LMP_{T,k}$ representing the total LMP or i can be C to represent the congestion component $LMP_{C,k}$ for time interval k at the node. The timeline under consideration is discretized to T time intervals of size Δ_T, which, in this case, is 1 h. $P_{ch,k}$ and $P_{dch,k}$ are the charging and discharging power of the BEV at time interval k. CF_{deg} is the constant degradation cost factor of the BEV battery. The cost of charging/discharging the energy from the BEV and/or the prevented congestion-related costs are incorporated in this objective.

Equations (10)–(19) represent the constraints of the optimization model. Equation (10) is based on the law of conservation of energy—it states that the energy stored in the BEV at time k depends on the energy in the BEV at time $(k-1)$, energy expenditure due to driving in time k, as well as the power flow into or out of the BEV at time k when plugged in. The BEV can be charged with power $P_{ch,k}$ with efficiency η_{ch}, discharged with power $P_{dch,k}$ with efficiency η_{dch}, or the BEV consumes power $P_{driv,k}$ when driven at time interval k. $P_{driv,k}$ is randomly set in the range of 5 to 10 kW to reflect a driven distance in the range of 15 to 30 miles but is fixed at that value for a given scenario. Both η_{ch} and η_{dch} are set at 90%. Equation (11) sets limitations on the maximum and minimum energy stored in the battery of the BEV. The energy in the BEV at any time interval k is assumed to lie between 10% (E_{min}) and 90% (E_{max}) of the BEV battery's rated capacity E^{rat}. Equations (12) and (13) set the charging and discharging power limitations of the BEV as $P_{ch,max}$ and $P_{dch,max}$, respectively, which, in this case, is 6.6 kWh. $\delta_{ch,k}$ and $\delta_{dch,k}$ are binary decision variables as shown in Equations (14) and (15). When $\delta_{ch,k}$ equals 1, the BEV is charging, and when it equals 0, the BEV is not charging. The same rule applies to $\delta_{dch,k}$. The sum of $\delta_{ch,k}$ and $\delta_{dch,k}$ is always less than or equal to 1, as shown in Equation (16), ensuring that the BEV can either charge, discharge, or remain idle when plugged in. Equations (17) and (18) ensure that the BEV cannot charge or discharge during the time intervals when it is driven. Equation (19)

states that the BEV must hit a minimum amount of energy $E_{dep,k}$ before its departure from a charging station.

The optimization is set up and solved using the gurobipy module in Python [48]. The only input data to the program are the LMP_T and LMP_C data of the nodes for the months of March 2021 to September 2023. The other parameters are set as stated in the assumptions. The outputs obtained are the average maximum revenue from the BEV, the congestion-related savings, the charging schedule of the BEV, the total discharged power, benefit per kWh of V2G, and battery degradation as capacity loss.

3. Results

In this section, we will first look at the total benefits from V2G-enabled BEVs at each node. Following this, we will explore seasonality and the behavior of BEVs at smaller time scales in these nodes.

The blue bars in Figure 4 shows the total savings (or revenue) earned by a single BEV at each node that participates in energy arbitrage with LMP_T pricing. The orange bars in the figure represent the congestion savings as an outcome of minimizing total charging cost. We can see that in each of the nodes, the BEV earns over 200 dollars, with a maximum of \$290.37 at node HURON_6_N001. However, the congestion savings are only in the range of 110–190 dollars for these nodes.
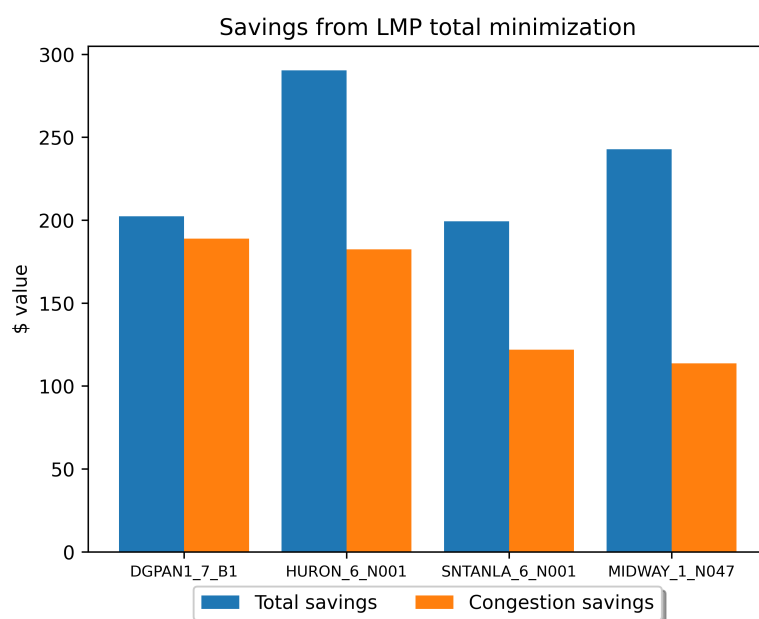
Figure 4. Savings from LMP_T minimization at the nodes at the ends of the transmission lines.

The results of the LMP_C optimization in Figure 5 shares an interesting find. Here, the blue bars show the total congestion savings by a single BEV at the appropriate node that participates in congestion minimization with LMP_C pricing. The orange bars represent the minimized total congestion costs. We see that congestion minimization comes at a significant cost based on the current market design. In each of the nodes, we can see congestion savings over \$380, except for one node at \$259.8. However, based on the current electricity market design, the BEVs have to pay in the range of \$670–950 to help minimize local congestion. This is one of the main reasons why BEVs with V2G capability will not participate in local congestion minimization with the current LMP pricing, unless they can be incentivized to do so.
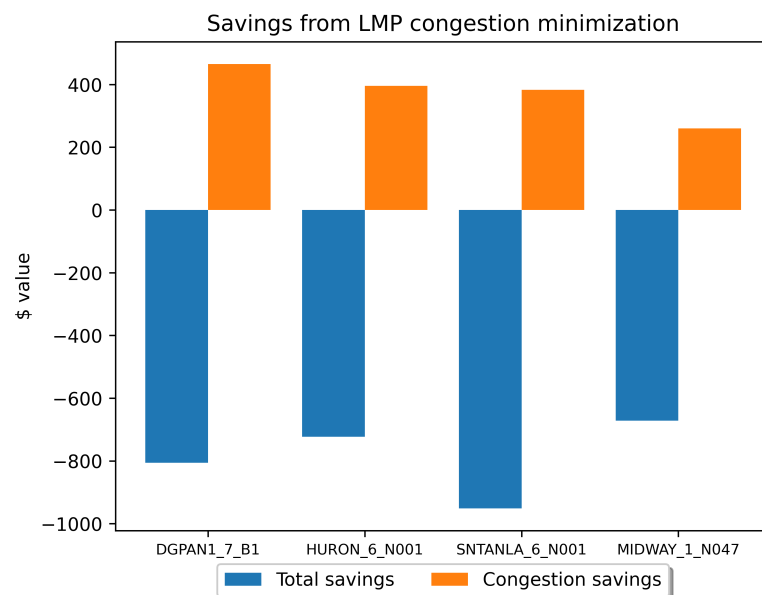
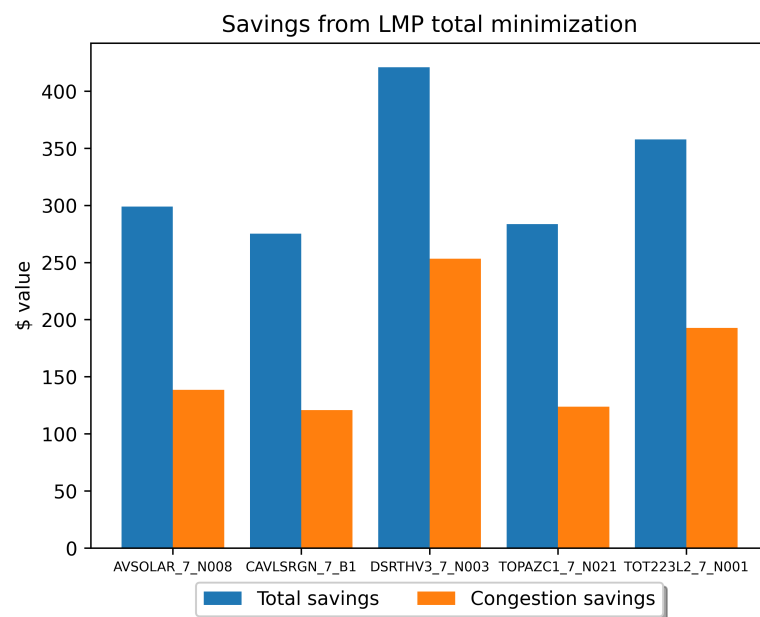**Figure 5.** Savings from LMP_C minimization at the nodes at the ends of the transmission lines.

The blue and orange bars in Figure 6 show the capacity degradation from the LMP_T and LMP_C optimization, respectively. The capacity losses for the LMP_T optimization are in the range of 3.7–3.8% for the timeline in consideration (March 2021 to September 2023), while the capacity losses for the LMP_C optimization are less than 2.7%. This suggests that the BEV discharges in fewer instances for the LMP_C optimization when compared to the LMP_T optimization.
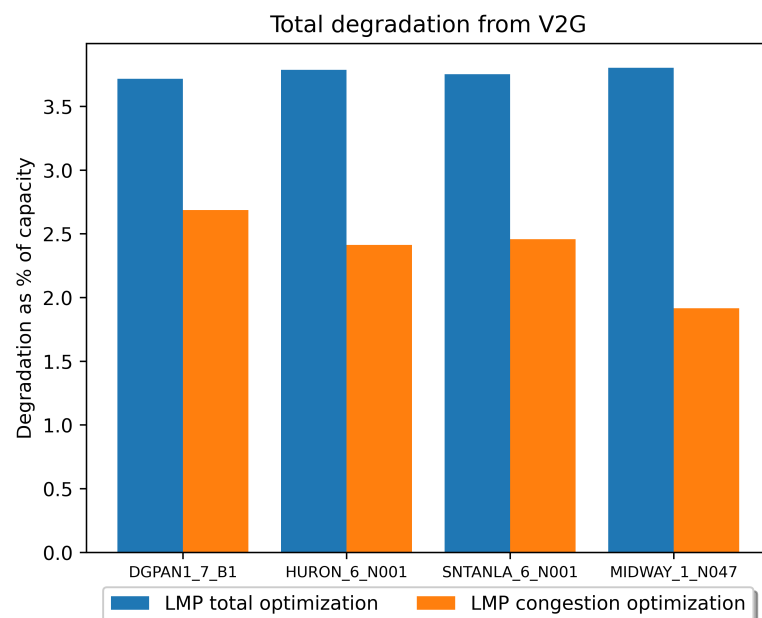
Figure 6. Battery capacity loss (%) from LMP_T and LMP_C minimization at the nodes at the ends of the transmission lines.

The blue bars in Figure 7 shows the total savings (or revenue) earned by a single BEV at each solar power plant node that participates in energy arbitrage with LMP_T pricing. The orange bars in the figure represent the congestion savings. We can see that in each of the cases, the BEV earns over 275 dollars, with a maximum of $420.1 at node DSRTHV3_7_N003. However, the congestion savings are only in the range of 120–255 dollars.

Figure 7. Savings from LMP_T minimization at the solar power plant nodes.

Figure 8 shares a similar finding as Figure 5. Here, the blue bars show the total savings earned by a single BEV at the appropriate node that participates in congestion minimization with LMP_C pricing. The orange bars represent the minimized total congestion costs. We can observe congestion savings in the range of $150–290 depending on location. However, the BEVs have to pay in the range of $400–660 to help minimize local congestion. This again shows that local congestion minimization may come at a cost to earning revenue from total LMP and highlights the need to incentivize action at a nodal level.
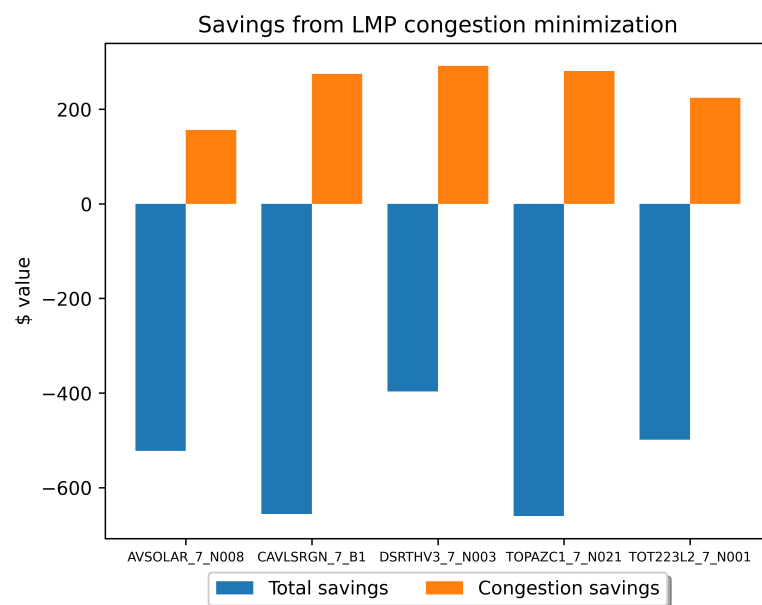
Figure 8. Savings from LMP_C minimization at the solar power plant nodes.

The blue and orange bars in Figure 9 show the capacity degradation from the LMP_T and LMP_C optimization, respectively, at the solar power plant nodes. The capacity losses for the LMP_T optimization are close to 3.8% for the timeline in consideration (March 2021 to September 2023), while the capacity losses for the LMP_C optimization are around 1.7–2%.
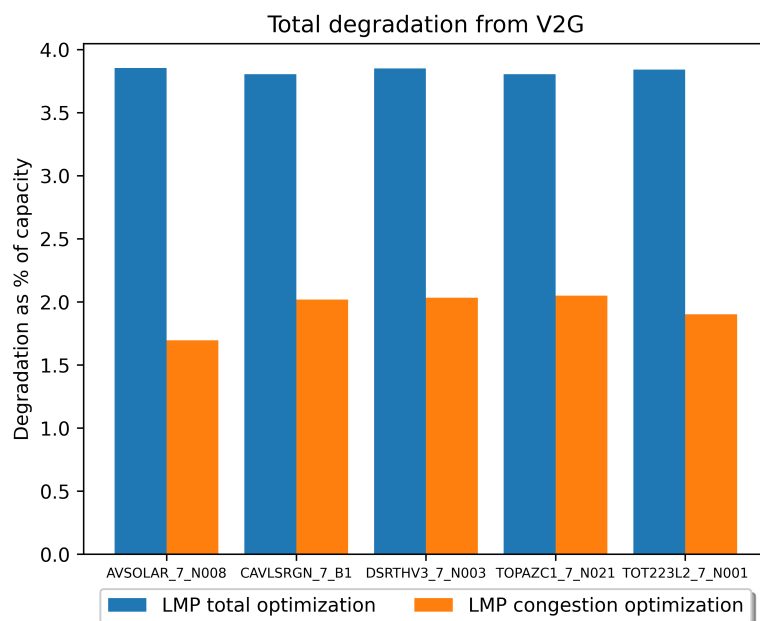
Figure 9. Battery capacity loss (%) from LMP_T and LMP_C minimization at the solar power plant nodes.

For conciseness, we focus on the nodes whose LMPs were highlighted in Figures 1–3 to observe the monthly trends in BEV behavior. The monthly distribution of arbitrage revenue and congestion savings from both the LMP_T and LMP_C optimization as well as the distribution of V2G commitment and degradation from nodes DGPAN1_7_B1, HURON_6_N001, and DSRTHV3_7_N003 are discussed below.

Figures 10–12 show the monthly distribution of revenue or congestion savings. A BEV optimized for LMP_T at DGPAN1_7_B1 can earn over \$50 in the months of May 2022, September 2022, and April 2023, but the congestion savings are much larger in May 2022 and April 2023 compared to September 2022. This shows that the LMP_T optimal charging strategy for a BEV results in both higher earnings and congestion savings during the spring season, but during summer, there is an opportunity to earn a higher amount with minimal influence on congestion. We also see that during the winter months, the congestion savings are higher than the revenue from arbitrage. This indicates a lower opportunity to earn revenue from arbitrage during winter. A drastic example in this case is during the months of December 2022 and January 2023, where \$84 and \$49 are required to charge the BEVs. Figure 11 shows a similar promise with higher earnings (greater than \$40) in the months of May 2022, September 2022, and April 2023, but congestion savings peak mostly during the spring months (though the value is much lower). Here again, the congestion savings are higher than the revenue from arbitrage during the winter months. We see a similar outcome for the solar power plant node DSRTHV3_7_N003 in Figure 12, showing potential earnings in May 2022, September 2022, and April 2023 being greater than \$35. However, we see that the revenue continues to remain high except for a dip in June 2023. We also see that the congestion savings are higher one month earlier compared to nodes DGPAN1_7_B1 and HURON_6_N001.
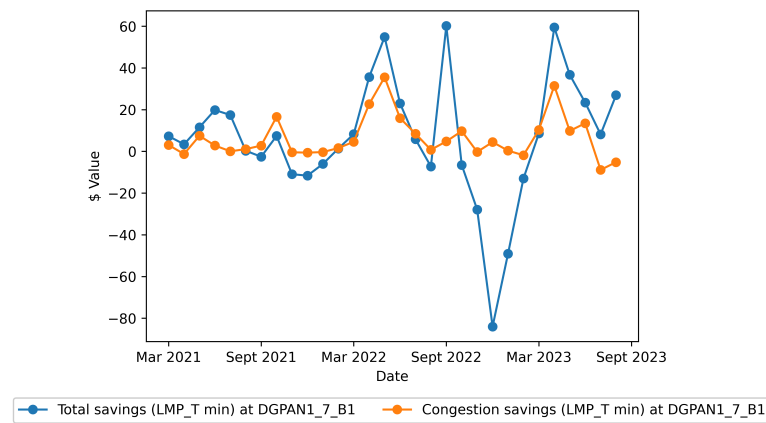
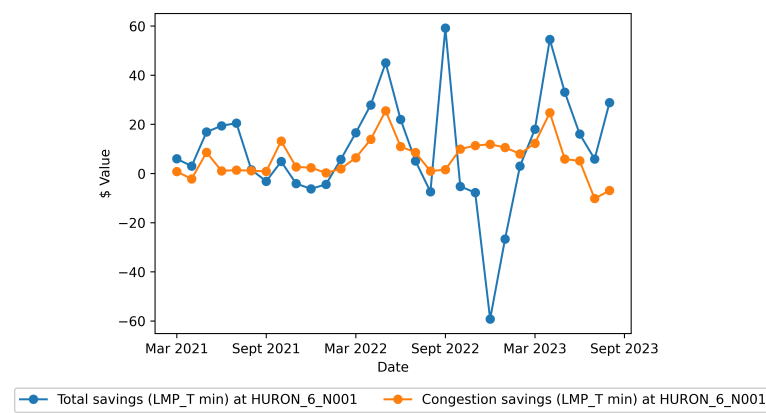**Figure 10.** Monthly savings from LMP_T minimization at DGPAN1_7_B1.

Figure 11. Monthly savings from LMP_T minimization at HURON_6_N001.
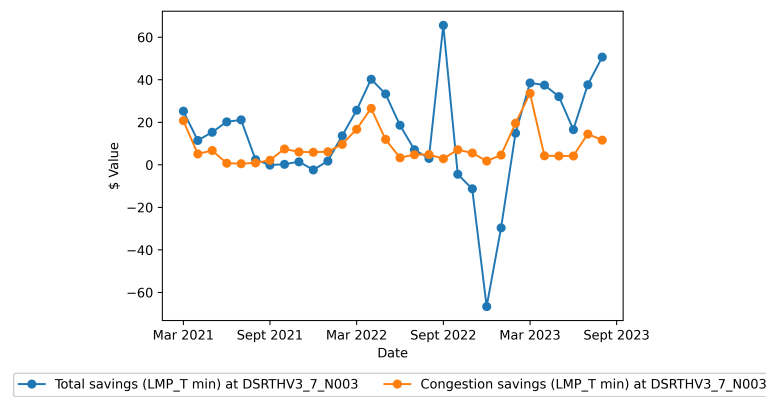

Figure 12. Monthly savings from LMP_T minimization at DSRTHV3_7_N003.

Figures 13–15 show the monthly distribution of revenue or congestion savings under LMP_C optimization. As seen previously, LMP_C minimization results in congestion savings but significantly increases charging costs. In both DGPAN1_7_B1 and HURON_6_N001, the congestion savings spike close to the months of April and May each year. During these months, the charging costs are not significant as well. However, for most other months from early summer to early spring, there are negligible congestion savings for a very large rise in charging costs, especially during December 2022, with charging costs as high as $174 and $117 in DGPAN1_7_B1 and HURON_6_N001, respectively. We see a similar trend with the solar power plant node DSRTHV3_7_N003. In the case of DGPAN1_7_B1 and HURON_6_N001, congestion minimization leads to revenue on the order of $8 and above (up to $35) for the months of April and May 2022 and 2023. The positive revenue

for DSRTHV3_7_N003 shows up in March 2021, March–April 2022, March 2023, and July–August 2023.
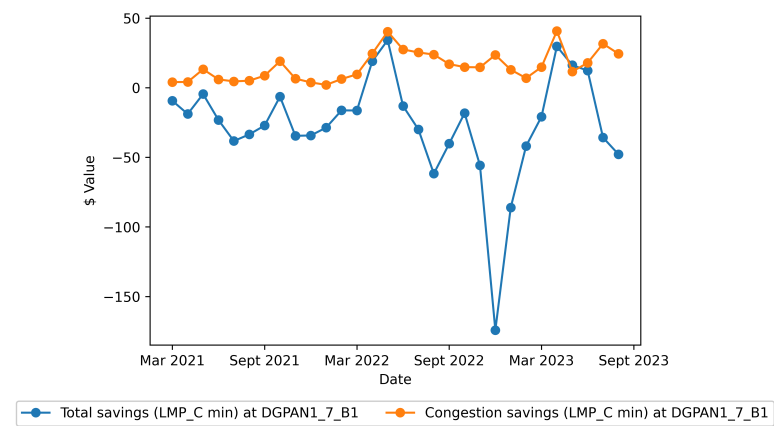

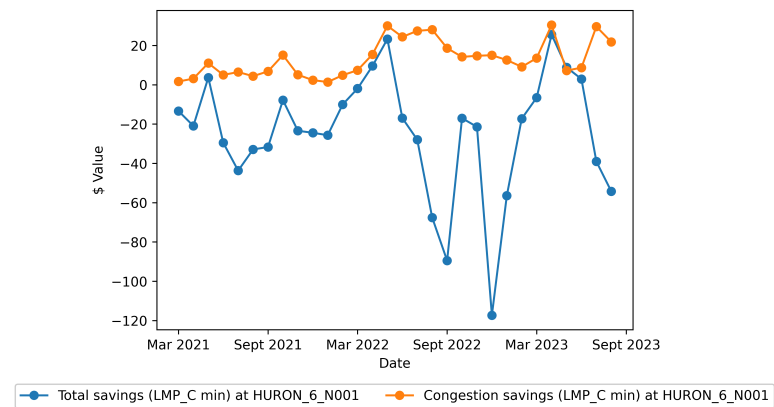**Figure 13.** Monthly savings from LMP_C minimization at DGPAN1_7_B1.

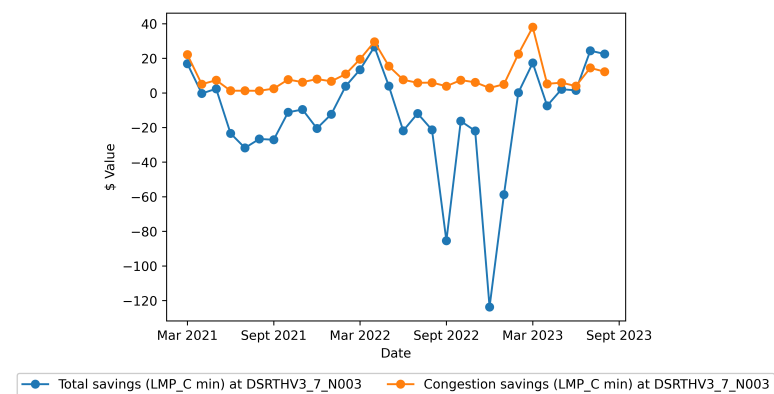**Figure 14.** Monthly savings from LMP_C minimization at HURON_6_N001.

Figure 15. Monthly savings from LMP_C minimization at DSRTHV3_7_N003.

Figures 16–18 show the total amount of V2G throughput provided by the BEV at the node for both LMP_T and LMP_C optimization. For the three nodes with LMP_T optimization, the V2G throughput is in the range of 500–900 kWh per month, with the exception of the months from October 2022 to January 2023 for DGPAN1_7_B1. For the three nodes with LMP_C optimization, the V2G throughput is in the range of 0–600 kWh per month, with the exception of the months from November 2022 to January 2023, where it is closer to 800 kWh for DGPAN1_7_B1 and HURON_6_N001. With respect to LMP_C optimization, we see a much smaller throughput of V2G in the range of 0–250 kWh for the months of

June 2021 to March 2022, with an exception in October 2021, as well as from January 2023 to March 2023 for all three nodes. Additionally, in DSRTHV3_7_N003, we see a low V2G throughput from September 2022 to June 2023, with an exception in March 2023.
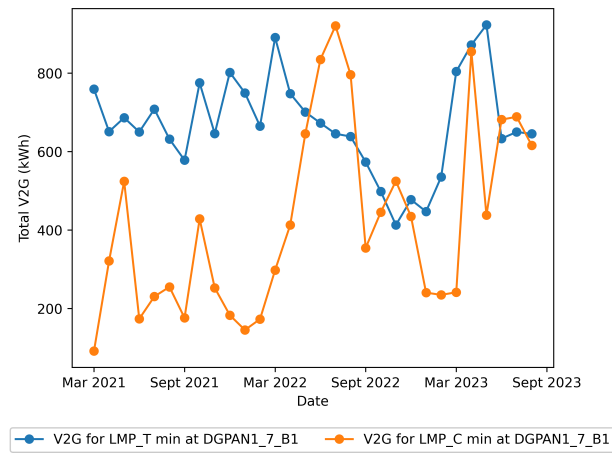

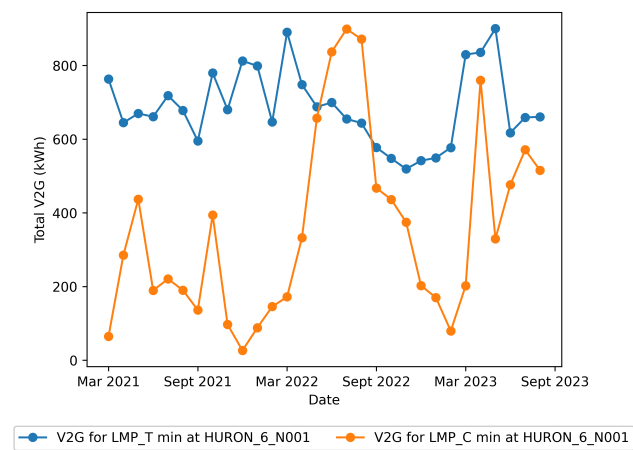**Figure 16.** Monthly total V2G power throughput at DGPAN1_7_B1.

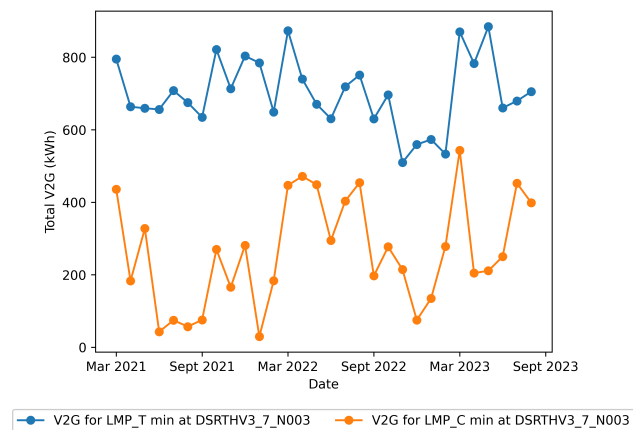**Figure 17.** Monthly total V2G power throughput at HURON_6_N001.

Figure 18. Monthly total V2G power throughput at DSRTHV3_7_N003.

Figures 19–21 show the value of congestion savings per units of V2G provided by the BEV at the nodes for both LMP_T and LMP_C minimization. We see a seasonal variation for the benefits per unit of V2G. As expected, the congestion savings from LMP_C minimization are higher than those from LMP_T minimization since the focus is to reduce congestion in

the former optimization. In all the cases, the benefits from LMP_C minimization are positive, but for some months, LMP_T optimization increases congestion, like July and August 2023 in DGPAN1_7_B1 and HURON_6_N001. The value from LMP_C optimization is in the range of 0.01–0.07 \$/kWh for most months for the three nodes. While no exceptions are seen at DGPAN1_7_B1, we observe a higher value (upto \$0.12/kWh) at HURON_6_N001 in the months of December 2021 and December 2022 to March 2023 and a very large spike in DSRTHV3_7_N003 in the month of January 2022, with a value of \$0.23/kWh.
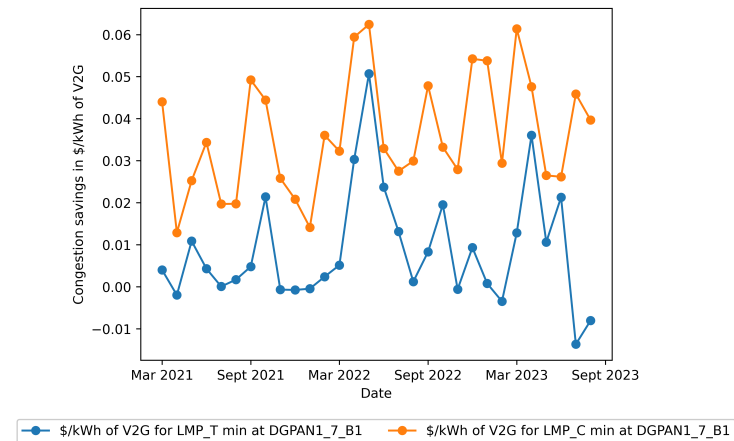

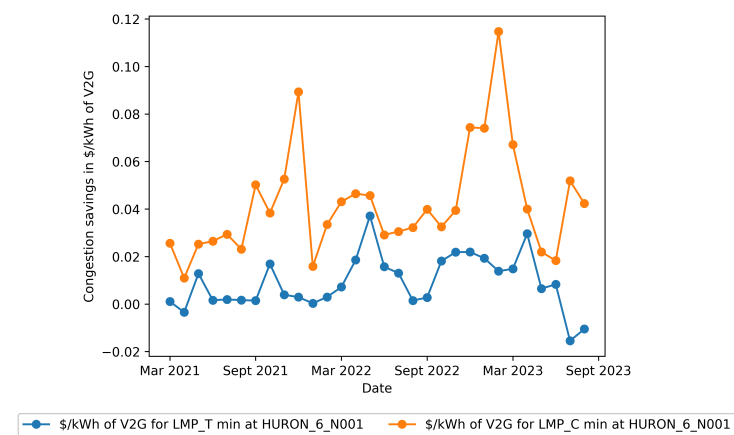**Figure 19.** Congestion savings in \$/kWh of V2G at DGPAN1_7_B1.

Figure 20. Congestion savings in \$/kWh of V2G at HURON_6_N001.
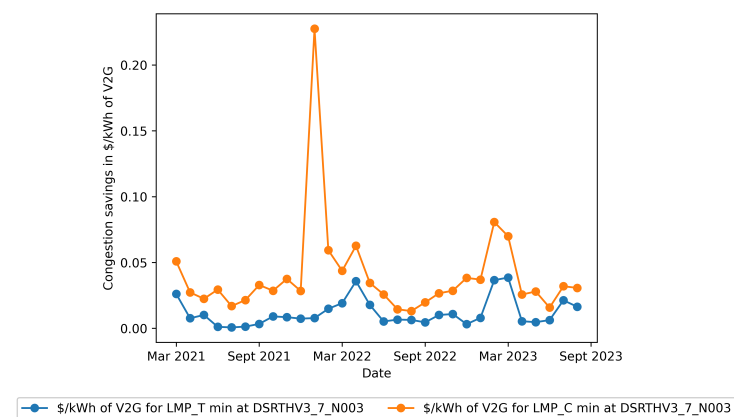

Figure 21. Congestion savings in \$/kWh of V2G at DSRTHV3_7_N003.

The other nodes listed in Tables 2 and 3 show similar findings as reported for DG-PAN1_7_B1, HURON_6_N001, and DSRTHV3_7_N003. We show that local congestion at nodes can potentially be minimized using BEVs and V2G with LMP_C minimization. The benefits seem to be larger during certain months of the year. Strong incentives to utilize V2G for congestion minimization could lead to lower stress on the grid and minimize sustainable energy curtailment and pollution.

4. Discussion

In this study, our initial focus centers on electric grid congestion and the utilization of FTRs as a means to mitigate price uncertainties that arise due to the inability of certain locations to use closer sustainable sources of energy due to transmission congestion. The large amounts of RES installed in the grid to combat climate change and air pollution are intermittent in nature, leading to frequent supply–demand mismatch and price fluctuations with the existing transmission infrastructure and electricity markets. We delve into the shortcomings of FTR markets, emphasizing that they are not a universal remedy for all transmission congestion challenges. Furthermore, we explore the application of utility-scale energy storage to alleviate transmission issues, while also considering the potential advantages of V2G technology in minimizing local congestion. We subsequently delve into the elements of LMPs and explore the potential utility of the congestion component in mitigating congestion, sustainable energy curtailment, and environmental pollution.

We identified three of the most congested transmission lines within CAISO and designated the nodes at the end of these lines as potential focal points for our analysis. Additionally, we factored in the nodes representing several of California's largest solar power facilities. Subsequently, we outline the approach for quantifying battery degradation using a constant degradation cost factor, which can be incorporated into our optimization program's objectives. Our next step involved developing optimization programs that incorporate either the total LMP LMP_T or the congestion component of LMP LMP_C within their objective functions.

We discovered that optimizing for LMP_T leads to revenue for the BEVs, along with some accompanying congestion savings. In contrast, optimizing for LMP_C yielded more substantial congestion savings but also led to a significant rise in the charging expenses for the BEVs. For the time period from March 2021 to September 2023, LMP_T optimization results in the BEV earning in the range of \$200–290 at the transmission line nodes and \$275–420 at the solar power plant nodes. However, the congestion savings are only in the range of \$110–190 and \$120–255 for the transmission line and the solar power plant nodes, respectively. In the case of LMP_C optimization, the congestion savings are in the range of \$260–430 and \$150–290 for the transmission line and the solar power plant nodes, respectively. However, the BEVs have to pay in the range of \$670–950 and \$400–660 for the transmission line and the solar power plant nodes, respectively, to help minimize local congestion. Local congestion minimization seems to come at a large increase in charging cost from total LMP and highlights the need to incentivize action at a nodal level. We also see that among the nodes chosen, the solar power plant nodes reflect greater revenue from arbitrage with LMP_T optimization; however, the congested transmission line nodes showcase significantly greater congestion savings with LMP_C minimization. The capacity losses for the BEV batteries from LMP_T optimization are in the range of 3.7–3.8% for all nodes, while the capacity losses for LMP_C optimization are in the range of 1.8–2.7% for transmission line nodes and 1.7–2% for the solar power plant nodes. This suggests that the BEV discharges in significantly fewer instances for LMP_C optimization when compared to LMP_T optimization, and the BEV performs V2G actions more often for the congested transmission line nodes.

Furthermore, we delved into the monthly breakdown of charging costs, revenue, congestion savings, and V2G throughput for both LMP_T and LMP_C optimization. This analysis sheds light on the seasonal variability of congestion and curtailment. While looking at the monthly distribution of revenue or congestion savings, we see that the LMP_T

optimal charging strategy for a BEV results in both higher earnings and congestion savings during spring months, but during summer, there is an opportunity to earn higher with minimal influence on congestion. We also see that during the winter months, the congestion savings are higher than the revenue from arbitrage, indicating a smaller opportunity to earn from arbitrage during winter. In the case of the solar power plant node, we see that the congestion savings are higher one month earlier compared to the transmission line nodes. LMP_C minimization results in congestion savings but significantly increases charging costs. The congestion savings are high during late spring/early summer with low charging costs. However, for most other months from early summer to early spring, there are negligible congestion savings for a very large rise in charging costs. The V2G throughput for LMP_C optimization is lower than that of LMP_T optimization for the transmission line nodes for most of the time period, with the exception of May–July 2022, which could indicate frequent transmission congestion in these months. The BEV at the solar power plant node always participated in more V2G for LMP_T optimization. We also clearly see that the congestion savings from LMP_C optimization is always greater than that from LMP_T optimization. However, there are a few months where the \$/kWh value from LMP_C optimization is significantly larger than the LMP_T counterpart, and this depends on both the location and the month.

These findings on the total benefits of V2G-enabled BEVs at different nodes, including financial savings and congestion cost reductions, highlight spatio-temporal patterns in local congestion. This work provides another lens to evaluate the value of V2G in a real-world context to alleviating congestion, in addition to other V2G services like frequency regulation, voltage regulation, energy arbitrage, and so on. We hope that this work helps in the push towards the automotive industry and government entities embracing V2G, and the launch of more V2G-enabled car models and charging stations, leading to a more sustainable planet. The battery degradation and capacity losses due to V2G participation were also studied to observe the trade-off between benefits and the longevity of BEV batteries.

Investigating the detailed correlation between different battery degradation models and the computed costs/savings is a potential idea for future work. There are multiple battery degradation models in the literature, and it will be very interesting to study the sensitivity of V2G operations on battery degradation costs. Another promising avenue for future research could involve investigating the implementation of a variable battery degradation cost factor in the context of LMP_C optimization, particularly given that LMP_C is notably lower than LMP_T in most instances. Initial attempts at utilizing a straightforward ratio of LMP_C/LMP_T multiplied by a constant degradation factor resulted in suboptimal outcomes due to occasional negative or near-zero prices of LMP_T. It is worth considering optimizing for the ratio of the monetary benefit to V2G throughput rather than monetary benefits alone. A mechanism could be devised to ensure that V2G actions are taken only when the benefits exceed a predefined threshold ratio, with the aim of minimizing battery degradation while maximizing the overall advantages.

This study highlights that prioritizing LMP_C optimization effectively reduces congestion costs. This, in turn, indirectly leads to diminished congestion, renewable energy curtailment, and pollution. However, it comes at the expense of higher charging costs in the present electricity markets. Typically, energy arbitrage with non-grid-scale storage is aligned with TOU pricing rather than LMP. A potential future research endeavor might investigate incentives and congestion-driven pricing at the distribution level to influence BEV user behavior to alleviate transmission congestion. This compensation approach becomes particularly vital for addressing challenges like aggregator fees, mitigating battery degradation, and discouraging participation in other V2G applications when congestion relief takes precedence.

Exploring the involvement of higher-power charging and the integration of BEVs with larger capacities, such as heavy-duty electric trucks and buses, in this context could offer intriguing insights. Given that nodes along congested transmission lines are occasionally located near freeways (as seen in this study with the congested lines running parallel and in

close proximity to the I-5 freeway), electric trucks have the potential to charge and discharge strategically at specific times and locations to alleviate congestion. The advantages of such an approach are likely to exhibit seasonal variations, and the application of innovative pricing mechanisms may encourage trucks to follow slightly adjusted routes for optimizing local energy supply and demand within the electric grid.

Abbreviations

The following abbreviations are used in this manuscript:

BEV	Battery Electric Vehicle
V2G	Vehicle-to-Grid
LMP	Locational Marginal Price
CAISO	California Independent System Operator
RES	Renewable Energy Sources
BESS	Battery Energy Storage System
ISO	Independent System Operator
RTO	Regional Transmission Organization
BTM	Behind-the-meter
PV	Photovoltaic
TOU	Time-of-use
DAM	Day-Ahead Market
RTM	Real-Time Market
GHG	Greenhouse gas
NHTA	National Household Travel Survey
PJM	Pennsylvania Jersey Maryland RTO
SPP	Southwest Power Pool
TCC	Transmission Congestion Contracts
CRR	Congestion Revenue Rights
DOE	Department of Energy
RTOD	Real Time Optimal Dispatch
TCR	Transmission Congestion Relief
MILP	Mixed Integer Linear Program

References

1. Priessner, A.; Hampl, N. Can product bundling increase the joint adoption of electric vehicles, solar panels and battery storage? Explorative evidence from a choice-based conjoint study in Austria. *Ecol. Econ.* **2020**, *167*, 106381. [CrossRef]
2. Edelenbosch, O.Y.; Hof, A.F.; Nykvist, B.; Girod, B.; Van Vuuren, D.P. Transport electrification: The effect of recent battery cost reduction on future emission scenarios. *Clim. Chang.* **2018**, *151*, 95–108. [CrossRef]
3. Sufyan, M.; Rahim, N.A.; Aman, M.M.; Tan, C.K.; Raihan, S.R.S. Sizing and applications of battery energy storage technologies in smart grid system: A review. *J. Renew. Sustain. Energy* **2019**, *11*, 014105. [CrossRef]
4. Fitzgerald, G.; Mandel, J.; Morris, J.; Touati, H. *The Economics of Battery Energy Storage: How Multi-Use, Customer-Sited Batteries Deliver the Most Services and Value to Customers and the Grid*; Rocky Mountain Institute: Basalt, CO, USA, 2015; Volume 6.

5. Rezaeimozafar, M.; Monaghan, R.F.; Barrett, E.; Duffy, M. A review of behind-the-meter energy storage systems in smart grids. *Renew. Sustain. Energy Rev.* **2022**, *164*, 112573. [CrossRef]

6. Li, T.; Tao, S.; He, K.; Lu, M.; Xie, B.; Yang, B.; Sun, Y. V2G multi-objective dispatching optimization strategy based on user behavior model. *Front. Energy Res.* **2021**, *9*, 739527. [CrossRef]

7. Sevilla, F.R.S.; Parra, D.; Wyrsch, N.; Patel, M.K.; Kienzle, F.; Korba, P. Techno-economic analysis of battery storage and curtailment in a distribution grid with high PV penetration. *J. Energy Storage* **2018**, *17*, 73–83. [CrossRef]

8. Gowda, S.N.; Ahmadian, A.; Anantharaman, V.; Chu, C.C.; Gadh, R. Power Management via Integration of Battery Energy Storage Systems with Electric Bus Charging. In Proceedings of the 2022 IEEE Power & Energy Society Innovative Smart Grid Technologies Conference (ISGT), New Orleans, LA, USA, 24–28 April 2022; IEEE: Piscataway, NJ, USA, 2022; pp. 1–5.

9. Englberger, S.; Jossen, A.; Hesse, H. Unlocking the potential of battery storage with the dynamic stacking of multiple applications. *Cell Rep. Phys. Sci.* **2020**, *1*, 100238. [CrossRef]

10. Gusev, Y.P.; Subbotin, P. Using battery energy storage systems for load balancing and reactive power compensation in distribution grids. In Proceedings of the 2019 International Conference on Industrial Engineering, Applications and Manufacturing (ICIEAM), Sochi, Russia, 25–29 March 2019; IEEE: Piscataway, NJ, USA, 2019; pp. 1–5.

11. Ma, H.; Balthasar, F.; Tait, N.; Riera-Palou, X.; Harrison, A. A new comparison between the life cycle greenhouse gas emissions of battery electric vehicles and internal combustion vehicles. *Energy Policy* **2012**, *44*, 160–173. [CrossRef]

12. Van Vliet, O.; Brouwer, A.S.; Kuramochi, T.; van Den Broek, M.; Faaij, A. Energy use, cost and CO2 emissions of electric cars. *J. Power Sources* **2011**, *196*, 2298–2310. [CrossRef]

13. McGuckin, N.A.; Fucci, A. *Summary of Travel Trends: 2017 National Household Travel Survey*; US Department of Transportation, Federal Highway Administration: Washington, DC, USA, 2018.

14. Kempton, W.; Letendre, S.E. Electric vehicles as a new power source for electric utilities. *Transp. Res. Part D Transp. Environ.* **1997**, *2*, 157–175. [CrossRef]

15. Galus, M.D.; Vayá, M.G.; Krause, T.; Andersson, G. The role of electric vehicles in smart grids. *Wiley Interdiscip. Rev. Energy Environ.* **2013**, *2*, 384–400. [CrossRef]

16. Lopes, J.A.P.; Soares, F.J.; Almeida, P.M.R. Integration of electric vehicles in the electric power system. *Proc. IEEE* **2011**, *99*, 168–183. [CrossRef]

17. Sortomme, E.; El-Sharkawi, M.A. Optimal charging strategies for unidirectional vehicle-to-grid. *IEEE Trans. Smart Grid* **2011**, *2*, 131–138. [CrossRef]

18. Gowda, S.N.; Eraqi, B.A.; Nazaripouya, H.; Gadh, R. Assessment and tracking electric vehicle battery degradation cost using blockchain. In Proceedings of the 2021 IEEE Power & Energy Society Innovative Smart Grid Technologies Conference (ISGT), Washington, DC, USA, 16–18 February 2021; IEEE: Piscataway, NJ, USA, 2021; pp. 1–5.

19. Denholm, P.; O'Connell, M.; Brinkman, G.; Jorgenson, J. *Overgeneration from Solar Energy in California. A Field Guide to the Duck Chart*; Technical Report; National Renewable Energy Lab. (NREL): Golden, CO, USA, 2015.

20. Sioshansi, R.; Denholm, P. Emissions impacts and benefits of plug-in hybrid electric vehicles and vehicle-to-grid services. *Environ. Sci. Technol.* **2009**, *43*, 1199–1204. [CrossRef]

21. Yu, H.; Niu, S.; Shang, Y.; Shao, Z.; Jia, Y.; Jian, L. Electric vehicles integration and vehicle-to-grid operation in active distribution grids: A comprehensive review on power architectures, grid connection standards and typical applications. *Renew. Sustain. Energy Rev.* **2022**, *168*, 112812. [CrossRef]

22. Inci, M.; Savrun, M.M.; Çelik, Ö. Integrating electric vehicles as virtual power plants: A comprehensive review on vehicle-to-grid (V2G) concepts, interface topologies, marketing and future prospects. *J. Energy Storage* **2022**, *55*, 105579. [CrossRef]

23. Rivera, S.; Kouro, S.; Vazquez, S.; Goetz, S.M.; Lizana, R.; Romero-Cadaval, E. Electric vehicle charging infrastructure: From grid to battery. *IEEE Ind. Electron. Mag.* **2021**, *15*, 37–51. [CrossRef]

24. Gowda, S.N.; Zhang, T.; Kim, C.J.; Gadh, R.; Nazaripouya, H. Transmission, Distribution deferral and Congestion relief services by Electric Vehicles. In Proceedings of the 2019 IEEE Power & Energy Society Innovative Smart Grid Technologies Conference (ISGT), Washington, DC, USA, 18–21 February 2019; IEEE: Piscataway, NJ, USA, 2019; pp. 1–5.

25. Byrne, R.H.; Nguyen, T.A.; Copp, D.A.; Chalamala, B.R.; Gyuk, I. Energy management and optimization methods for grid energy storage systems. *IEEE Access* **2017**, *6*, 13231–13260. [CrossRef]

26. Eyer, J.M.; Corey, G.P.; Iannucci, J.J., Jr. *Energy Storage Benefits and Market Analysis Handbook: A Study for the DOE Energy Storage Systems Program*; Technical Report; Sandia National Laboratories: Albuquerque, NM, USA, 2004.

27. Lyons, K.; Fraser, H.; Parmesano, H. An introduction to financial transmission rights. *Electr. J.* **2000**, *13*, 31–37. [CrossRef]

28. Rudkevich, A.M.; Caramanis, M.C.; Goldis, E.A.; Li, X.; Ruiz, P.A.; Tabors, R.D. Financial Transmission Rights in Changing Power Networks. In Proceedings of the 2016 49th Hawaii International Conference on System Sciences (HICSS), Koloa, HI, USA, 5–8 January 2016; IEEE: Piscataway, NJ, USA, 2016; pp. 2326–2334.

29. Hogan, W.W. Contract networks for electric power transmission. *J. Regul. Econ.* **1992**, *4*, 211–242. [CrossRef]

30. Ye, H.; Ge, Y.; Shahidehpour, M.; Li, Z. Uncertainty marginal price, transmission reserve, and day-ahead market clearing with robust unit commitment. *IEEE Trans. Power Syst.* **2016**, *32*, 1782–1795. [CrossRef]

31. Kristiansen, T. Markets for financial transmission rights. *Energy Stud. Rev.* **2004**, *13*, 25–74. [CrossRef]

32. Leslie, G.W. Who benefits from ratepayer-funded auctions of transmission congestion contracts? Evidence from New York. *Energy Econ.* **2021**, *93*, 105025. [CrossRef]

33. Del Rosso, A.D.; Eckroad, S.W. Energy storage for relief of transmission congestion. *IEEE Trans. Smart Grid* **2013**, *5*, 1138–1146. [CrossRef]

34. Khani, H.; Zadeh, M.R.D.; Hajimiragha, A.H. Transmission congestion relief using privately owned large-scale energy storage systems in a competitive electricity market. *IEEE Trans. Power Syst.* **2015**, *31*, 1449–1458. [CrossRef]

35. Arteaga, J.; Zareipour, H.; Amjady, N. Energy storage as a service: Optimal pricing for transmission congestion relief. *IEEE Open Access J. Power Energy* **2020**, *7*, 514–523. [CrossRef]

36. Nguyen, T. *DOE Global Energy Storage Database*; Sandia National Laboratories: Albuquerque, NM, USA, 2021.

37. Staudt, P.; Schmidt, M.; Gärttner, J.; Weinhardt, C. A decentralized approach towards resolving transmission grid congestion in Germany using vehicle-to-grid technology. *Appl. Energy* **2018**, *230*, 1435–1446. [CrossRef]

38. Asrari, A.; Ansari, M.; Khazaei, J.; Fajri, P. A market framework for decentralized congestion management in smart distribution grids considering collaboration among electric vehicle aggregators. *IEEE Trans. Smart Grid* **2019**, *11*, 1147–1158. [CrossRef]

39. California ISO, Monthly Market Performance Reports. Available online: https://www.caiso.com/Pages/DocumentsByGroup. aspx?GroupID=A9180EE4-8972-4F3B-9CB8-21D0809B645E (accessed on 10 September 2023).

40. California Energy Commission—California State Geoportal, California Electric Transmission Lines. Available online: https: //gis.data.ca.gov/datasets/260b4513acdb4a3a8e4d64e69fc84fee/explore (accessed on 15 September 2023).

41. California ISO, Today's Outlook—Price Map. Available online: https://www.caiso.com/TodaysOutlook/Pages/prices.html (accessed on 15 September 2023).

42. California Energy Commission—California State Geoportal, California Power Plants. Available online: https://cecgis-caenergy. opendata.arcgis.com/datasets/CAEnergy::california-power-plants/explore?location=37.174065%2C-118.394256%2C6.74 (accessed on 15 September 2023).

43. California ISO, Managing Oversupply. Available online: https://www.caiso.com/informed/Pages/ManagingOversupply.aspx (accessed on 15 August 2023).

44. Preis, V.; Biedenbach, F. Assessing the incorporation of battery degradation in vehicle-to-grid optimization models. *Energy Inform.* **2023**, *6*, 33. [CrossRef]

45. Farzin, H.; Fotuhi-Firuzabad, M.; Moeini-Aghtaie, M. A practical scheme to involve degradation cost of lithium-ion batteries in vehicle-to-grid applications. *IEEE Trans. Sustain. Energy* **2016**, *7*, 1730–1738. [CrossRef]

46. Naumann, M.; Spingler, F.B.; Jossen, A. Analysis and modeling of cycle aging of a commercial LiFePO4/graphite cell. *J. Power Sources* **2020**, *451*, 227666. [CrossRef]

47. Yue, Q.; He, C.; Wu, M.; Zhao, T. Advances in thermal management systems for next-generation power batteries. *Int. J. Heat Mass Transf.* **2021**, *181*, 121853. [CrossRef]

48. Gurobi Optimization, LLC. Gurobi Optimizer Reference Manual. Available online: https://www.gurobi.com/documentation/ current/refman/refman.html (accessed on 15 August 2023).